Journal of Aerosol Science 132 (2019) 60–69

Contents lists available at ScienceDirect

Journal of Aerosol Science

journal homepage: www.elsevier.com/locate/jaerosci

Hygroscopic growth of CsI and CsOH particles in context of nuclear reactor accident research

Gaurav Mishra[a], Anil Kumar Mandariya[b], S.N. Tripathi[b,*], Mariam[c], Manish Joshi[c], Arshad Khan[c], B.K. Sapra[c]

[a] Nuclear Engineering and Technology Programme, Department of Mechanical Engineering, IIT, Kanpur, 208 016, India
[b] Department of Civil Engineering, IIT, Kanpur, 208 016, India
[c] Radiological Physics and Advisory Division, Bhabha Atomic Research Centre, Mumbai, 400 085, India

ARTICLE INFO

Keywords:
Fission product aerosols
CsI
CsOH
Hygroscopic growth
HTDMA

ABSTRACT

Studies of behavioral characteristics of fission product aerosols are extremely important in context of suspected environmental release during a severe nuclear reactor accident. Fission product aerosols generated in such a case are expected to travel from coolant systems to the containment and may get released to the environment in the most unlikely scenario of containment breach. Presence of steam also affects their dynamic behaviour and fate. Interaction of aerosol particles with water vapor in subsaturation domain modifies their physical and chemical characteristics. The objective of this study was to examine the hygroscopic nature of nuclear accident relevant cesium bound compounds viz. CsI, CsOH with the use of Hygroscopic Tandem Differential Mobility Analyzer (HTDMA). The growth factors for single component aerosols were obtained for different initial size of particles at different relative humidity levels. Growth factor curves as well as deliquescent parameters for CsI and CsOH particles have been obtained for the first time and have a crucial role towards environmental source term estimations in the event of nuclear accident. Experimental results were also compared with the theories available in literature.

1. Introduction

Cesium gets emitted to atmosphere through activities e.g. terrestrial erosion, ore mining-milling etc. Once in air, it gets attached to the surfaces of existing aerosol particles (Kristiansen et al., 2016). Its dynamics and fate in the environment then is governed by the characteristics of the aerosol size spectrum. Depending on the mean size, cesium bound particles get transported (short and long range) and ultimately settle on the earth's surfaces. These particles contaminate water and soil due to their chemical and radiotoxicity. Their presence at high concentration has potential to affect the quality of the inhaled air as well. Biomass burning events provide another mechanism for the remobilization of cesium deposited on trees and plants (Paliouris, Taylor, Wein, Svoboda, & Mierzynski, 1995, pp. 153–166). An estimated 40–70% of the cesium in the biomass fuel gets released to the atmosphere during a typical field fire with release increasing with the temperature (Amiro, Sheppard, Johnston, Evenden, & Harris, 1996). The higher levels of cesium in northern ecosystems have been attributed to the cesium re-suspension from Boreal fire episodes (Paliouris et al., 1995, pp. 153–166).

In another domain, compounds (CsI, CsOH) of radioactive cesium (Cs-134, Cs-137) as fission product aerosols are/may get

* Corresponding author.
E-mail address: snt@iitk.ac.in (S.N. Tripathi).

https://doi.org/10.1016/j.jaerosci.2019.03.008
Received 9 May 2018; Received in revised form 23 January 2019; Accepted 23 March 2019
Available online 29 March 2019
0021-8502/ © 2019 Published by Elsevier Ltd.

released to the environment during nuclear detonations and nuclear reactor accidents (Buckle, 1991; Kugeler, Epping, & Roes, 1989). Due to the hazard they posses, these compounds are integral to probabilistic safety studies and source term estimations in context of nuclear reactor accident research. Various nuclear accident scenarios are analyzed with nuclear safety codes (Saraswat, Munshi, Khanna, & Allison, 2017; (Saraswat, Munshi, Khanna, & Allison, 2018). A total of 1.4% core mass consisting of structural materials (3%), control materials (73%) and fission products (24%) may get released in a severe nuclear reactor accident (Wichner & Spence, 1985). Fission product vapors such as CsI and tellurium released from breached fuel rods condense on the particles in cooler regions above the core (Petti, 1989). CsI in presence of steam in reactor sections may convert to CsOH and a combination of CsI and CsOH is expected to be retained in containment following severe accident conditions (Allelein, Auvinen, & Ball, 2009; Jokiniemi, 1988). As a major component in reactor component, cesium affects the source term calculations for other compounds. 95% of iodine released in an event of reactor accident is assumed to be in the form of CsI (U. N. R. Commission, 2000). The large scale nature and severity of impacts of nuclear reactor accidents have been proven in terms of signatures such as spreading of radioactive plume over the northern hemisphere after Fukushima accident (Adachi Kouji & Mizuo, 2013; Leon et al., 2011). Some studies have also discussed the exposure of firefighters and general population from resuspended cesium on account of wildfires in areas near Chernobyl (Hao, Bondarenko, Zibtsev, & Hutton, 2008; Yoschenko et al., 2006). Radionuclides of cesium were also detected in huge amounts at various places, months after the Fukushima Daiichi Nuclear Power Plant accident (Long et al., 2012). Estimation of release amounts of cesium discharged into the atmosphere after nuclear reactor accidents has been discussed in detail in various studies (Adachi Kouji & Mizuo, 2013; Long et al., 2012; Nagai, Katata, Terada, & Chino, 2014, pp. 155–173). For example, after Fukushima Daiichi Nuclear Power Plant accident, a study was conducted by Stohl et al. (2012) at several dozen stations in Japan, North America and other regions, which reports a cesium activity release of 9–36 peta-becquerel(PBq) (Adachi Kouji & Mizuo, 2013; Stohl et al., 2012).

Evolution of aerosol size distribution via extrinsic processes (condensation, deposition etc.) and intrinsic modulations (e.g. coagulation) is linked with the fate of particles. Hygroscopic growth is another characteristic which plays crucial role in aerosol dynamics. In sub-saturation humidity levels, aerosol particles absorb or release vapor molecules governed by local saturation ratios. Precise information of hygroscopic growth of particles is crucial as it affects other parameters such as size, boiling point, droplet viscosity etc. Deposition rate of particles are expected to be affected at high RH (>90%) reflecting in increased settling rates. This enhancement is due to the increase in size after hygroscopic growth which gets reflected as higher gravitational settling velocities (Seinfeld and Pandis, 1998; Singh, Gupta, Tripathi, Jariwala, & Das, 2011). Aerosol particles released during nuclear power plant accidents include hygroscopic compounds in significant amount. These compounds in favorable conditions absorb water and hence have potential to grow in sub saturated conditions (Wichner & Spence, 1985). The growth in size further affects the dynamic characteristics (e.g. coagulation, condensation) and the source term in environment evolves with changing life-times of particles. A thorough study of the mechanisms of aerosol formation has been carried out by Petti (1989). He concluded that aerosol formation takes place rapidly (in less than 1–100 s) and the resulting particle size distribution can be calculated analytically by uncoupling vapor depletion from aerosol growth. Deliquescence relative humidity (DRH), threshold RH above which particles begin to absorb water or dissolve as solution, is also decisive parameter for depositional and transportation characteristics. Studies aimed at determining DRH and Efflorescence relative humidity (ERH i.e. point of recrystallization) rely on accurate measurements of particle size modifications with change in humidity levels (Cohen, Flagan, & Seinfeld, 1987; Jokiniemi, 1990; Tang, 1976). Several studies have been performed for studying the hygroscopic behaviour of various atmospheric relevant aerosols such as ammonium sulphate, sodium chloride, sodium nitrate, humic acid, succinic acid and dicarboxylic acids (Badger et al., 2006; Gysel, Weingartner, & Baltensperger, 2002; Peng, Chan, & Chan, 2001; Sjogren et al., 2007; Wex et al., 2008; Wise, Surratt, Curtis, Shilling, & Tolbert, 2003). Materials which include inorganic salts (e.g. ammonium sulphate, sodium chloride) showing step function form of critical points (DRH, ERH) and other electrolytes (e.g. sodium nitrate, malonic acid, glutaric acid) which absorb water at quite low RH (< 20%) showing continuous growth with humidity. Out of the techniques available for the measurement of hygroscopic growth factors (McMurry & Stolzenburg, 1989; Onasch et al., 1999; Tang & Munkelwitz, 1994) of aerosol particles, Hygroscopic Tandem Differential Mobility Analyzer (HTDMA) systems are most commonly used.

Although a lot of work has been performed for atmospheric relevant aerosol particles, essential knowledge of hygroscopic properties for important nuclear relevant aerosol particles does not exist. Accurate understanding of dynamic behaviour of crucial cesium compounds (CsI, CsOH) in aerosol phase is desirable. In literature, various properties (such as condensational growth, deposition) of cesium compounds are studied (Acquista, Abramowitz, & Lide, 1968; Badawi, Xerri, Canneaux, Cantrel, & Louis, 2012; Inada & Akagane, 1996; Kuczkowski, Lide, & Krisher, 1966; Li et al., 2013; McFarlane, Wren, & Lemire, 2002). but hygroscopic behaviour is a notable omission. Such an information is important for estimating/improving deposition fractions in coolant pipes (Modi et al., 2014), evolution in containment atmosphere (Sapra et al., 2008) and source term to the environment in an event of severe nuclear reactor accident (Camata, Hirasawa, Okuyama, & Takeuchi, 2000). Moreover, it is also expected to supplement the predictive capability of numerical models against source term estimations and risk-hazard evaluations. In this study, the hygroscopic properties at different relative humidity of laboratory generated single salt CsI (cesium iodide) and CsOH (cesium hydroxide) aerosols were investigated. Growth curves in humid air for both salts, the deliquescence relative humidity (DRH) and efflorescence relative humidity (ERH) of CsI 100 nm particles were measured at room temperature (298 K). In addition, the growth factors of dry diameter 50, 100, 150 and 200 nm particles at different RH were also measured separately for both CsI and CsOH to verify the significance of the Kelvin effect during hygroscopic growth of these salts. A comparison of standard growth factor models with experimental observations is also presented.

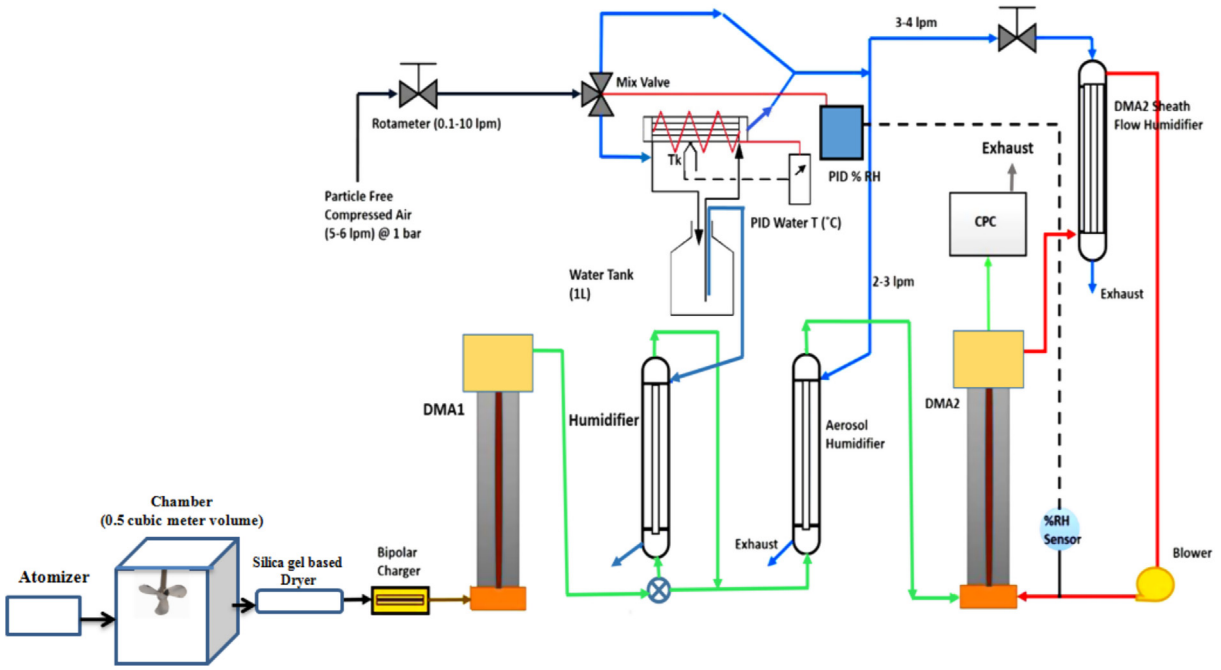

Fig. 1. Experimental setup

2. Experimental section and data analysis

The HTDMA system (experimental set-up and methodology) was used to determine the hygroscopic growth of CsI and CsOH particles. This system has been employed and discussed in detail in available literature (Gysel et al., 2004; Johnson, Fletcher, Meyer, Modini, & Ristovski, 2008; Villani, Picard, Michaud, Laj, & Wiedensohler, 2008; Weingartner, Gysel, & Baltensperger, 2002). The system for the current work was calibrated against the growth factors of laboratory generated salts (e.g. $NaCl$ or $(NH_4)_2SO_4$) (Gysel et al., 2002). Test solutes were dissolved in MilliQ water (typically 0.1 g/L, resistivity = $18.2M\Omega.\ cm$) and aerosolized through aerosol atomizer (TOPAS ATM 226). 0.1 M salt solutions (CsI, purity >99.5% ,Merck; CsOH, purity >99%, Merck) were used for this purpose. As shown in Fig. 1, the generated particles first entered into a fully clean chamber of 0.5 m^3 volume used for homogenization of generated aerosols. After 20–25 min, the steady state is achieved inside the chamber. Sample aerosol stream is subsequently passed through a silica gel based diffusion dryer in order to dry the sample to RH <15% at 298 K. This dryer has also been used in our previous work in different contexts (Mariam, Khandare, Koli, & KhanSapra, 2017; Shamjad et al., 2012). Most of the aerosol particles are expected to possess unit growth factors below this limiting RH (Villani et al., 2008). The dry aerosol stream is brought to charge conditioner (TSI-3077) and then fed into the first differential mobility analyzer (DMA)(TSI DMA 3081) of the experimental setup. This DMA recorded the RH of the aerosol flow stream apart from selecting monodisperse particle size for humidification. Monodisperse aerosol stream is then entered to a humidifier system in which controlled and stable humidity is maintained using a nafion membrane (Perma Pure single tube MD-110-12S-4). Saturated air counter flow technique is used for regulating the humidity in the humidity control system, which is based on the machanism described by Villani et al. (2008).

Monodisperse aerosol particles were passed through membrane of humidifier with a maintained counter flow of saturated air outside it. Moisture from saturated air can diffuse through the membrane into the aerosol stream. The diameter and concentration of particles after equilibrium at a defined RH is then measured by the Scanning Mobility Particle Sizer (SMPS, TSI 3082) consisting of DMA (TSI 3081) and a condensation particle counter (CPC, TSI 3776). The RH of the second DMA sheath flow is adjusted independently using another sheath humidifier in which vertically oriented multiple nafion membranes (PermaPure multi-tube PH-60T-12SS) are used. In the sheath flow humidifier, saturated air flows through the interior of membranes in top to bottom order while sheath air passes through outside the membranes in counter flow manner to minimize pressure drop. The humidity of both the humidifiers is regulated using a Proportional-Integral-Derivative (PID) controller which compares the set point values of RH and temperature with those measured by the sensor (Rotronic, HC2 - P05). Both humidifiers maintain the same relative humidity equal to the provided set point.

For efflorescence relative humidity (ERH) determination (decreasing RH experiments), another humidifier system in which stable humidity is maintained using a nafion membrane (Perma Pure single tube MD-110-12S-4) just after the first DMA. Here also the saturated air counter flow technique is used for regulating the humidity, which is based on the machanism described by Villani et al. (2008). When the aerosol particles passes through it, they get exposed to a very high relative humidity of 97–98% RH. This high RH is sufficient to dissolve the salt particle completely, which is essential for the decreasing relative humidity behaviour study of the aerosols.

Hygroscopic growth of particles with diameter 50, 100, 150 and 200 nm has been measured in the humidity range of 20%–94% RH with an accuracy of ± 1% RH employing above discussed experimental setup. The growth factor measurement accuracy depends on the uncertainty in controlling and measuring RH (Gysel, McFiggans, & Coe, 2009). Necessary protocols, due calibration procedures including offset calibration are followed during these experiments. All the data collected with this experimental setup is then corrected with TDMAinv toolkit developed by Gysel et al. (2009). This inversion algorithm uses a full TDMA kernel function and it also approximates the inverted growth factor probability density function (GF-PDF) as a piecewise linear function (Duplissy et al., 2009; Gysel et al., 2009). The relative humidity inside the second DMA varies little around the fixed target value which causes a simultaneous variability in measured growth factors. So the measurements within a range of ± 2% of target RH were considered for that particular RH and growth factors were recalculated according to the approach suggested by Gysel et al. (2009).

3. Theoretical approach

The Kohler theory (Kohler, 1936), which describes the growth of aqueous solution droplets in humid air is described in detail in Seinfeld and Pandis (1998). The Kohler equation (equation (1)) is based on a combination of two expressions: the Kelvin equation and modified Roult's law. Kelvin term governs the increase in water vapor pressure over a curved surface while modified Roult's law term describes solute effect that tends to decrease vapor pressure over a solution droplet.

$$\ln \frac{P_w(D_p)}{P^0} = \frac{4M_w\sigma_w}{RT\rho_w D_p} - \frac{6v_s n_s M_w}{\pi\rho_w D_p^3} \tag{1}$$

where $P_w(D_p)$ is the water vapor pressure over the droplet of diameter D_p, P^0 is the water vapor pressure over a flat surface at the same temperature, σ_w is the surface tension of droplet, ρ_w is the density of pure water, M_w is the molecular weight of pure water, n_s is number of moles of solute, R is the universal gas constant, T is the temperature in kelvin, ρ is density of salt and v_s is the number of ions generated by dissociation of a molecule of salt. The saturation ratio (S) and the two constants A_w and B_s can be defined as:

$$S = \frac{P_w(D_p)}{P^0}$$

$$A_w = \frac{4M_w\sigma_w}{RT\rho_w}$$

$$B_s = \frac{6v_s n_s M_w}{\pi\rho_w}$$

Then equation (1) can be rewritten as:

$$\ln S = \frac{A_w}{D_p} - \frac{B_s}{D_p^3} \tag{2}$$

There are several forms of Kohler equation (under differing approximations) presented in literature used for specific purposes (Facchini, Decesari, Mircea, Fuzzi, & Loglio, 2000; Shulman, Jacobson, Carlson, Synovec, & Young, 1996; Wex et al., 2008). The most frequently used form of equation (1), derived by Kohler (Pruppacher, Klett, & Wang, 1998) makes assumptions in addition to volume additivity, the solution is dilute, the activity coefficient of water can be assumed to be equal to 1 and the surface tension of the dilute solution can be approximated by that of pure water. Under these assumptions in equation (2), values of A_w and B_s are:

$$A_w \cong \frac{0.66}{T}$$

$$B_s \cong \frac{3.44*10^{13} v M_s}{M_w}$$

where the units of A_w and B_s are μm and μm^3 respectively.

A simpler form of Kohler model is proposed by Weingartner, Burtscher, and Baltensperger, (1997) and well explained by Brechtel and Kreidenweis (2000). This equation can also be used for predicting theoretical growth factors of single salt solutions. This equation reduces the need of surface tension and density data of the droplet at various concentrations. As the surface tension and density data is not known at higher molalities for the examined salts, this approach (Weingartner et al., 1997), Brechtel and Kreidenweis (2000) is adopted for theoretical predictions.

The model can be described in terms of relative humidity (RH) as:

$$RH = 100 \exp\left\{\frac{\alpha}{D_p}\right\} \exp\left\{\frac{\beta N_i}{D_0^3 - D_p^3}\right\} \tag{3}$$

where α is equal to 2.155 nm, β is equal to $5.712*10^{-2} nm^3$, the droplet size (D_p) and dry particle size (D_0) are in nanometers. The unknown parameter N_i (number of dissociated molecules in the water layer of droplet), can be defined by equation (4):

$$N_i = Y N_{av} (\pi/6) D_0^3 \tag{4}$$

where N_{av} is Avagadro's number and according to Brechtel and Kreidenweis (2000), Y can be calculated by using equation (5) in which ρ_s and M_s are density and molecular weight of solute respectively.

$$Y = \frac{v_s \rho_s}{M_s} \tag{5}$$

In another model Brechtel and Kreidenweis (2000), modified Kohler equation is developed in terms of parameters to be determined from HTDMA studies. The advantage of using this model is the parameterization of osmotic coefficient data itself. This model (equations (6)–(8))also assumes the surface tension of solution droplet same as that of pure water.

$$RH = 100 a_w \exp\left\{\frac{4\sigma_{drop}\overline{v_l}}{RTD_{drop}}\right\} \tag{6}$$

where RH is in percentage, $\overline{v_l}$ is partial molar volume of the solution, is surface tension of droplet, R is universal gas constant, T and D_{drop} are temperature and diameter of droplet respectively. a_w is the water activity and for aqueous solutions of ionic compounds, it can be defined as (Robinson & Stokes, 1968; Robinson & Stokes, 2012):

$$a_w = \exp\left\{\frac{-M_w \nu \phi m}{1000}\right\} \tag{7}$$

where M_w is the molecular weight of pure water, ν is total number of ions of salt present in solution, ϕ is osmotic coefficient of solution and m is molality of the solution.

Due to the unavailability of purely theoretical model, a semi empirical model is considered for calculating the osmotic coefficient (Clegg & Pitzer, 1992; Gysel et al., 2002; Pitzer, 1973; Pitzer & Mayorga, 1973)

$$\phi = 1 - |z_1 z_2| \left\{\frac{A_\phi I^{0.5}}{1 + b_{pit} I^{0.5}}\right\} + \frac{2\nu_1\nu_2}{\nu}\{\beta_0 + \beta_1 \exp(-\alpha I^{0.5})\}m + 2(\nu_1\nu_2)^{1.5} C_\phi m^2/\nu \tag{8}$$

where the value of α and β_{pit} are 2 and 1.2 at 298 K, respectively, z_1 and z_2 are charges on the ions respectively, ν_1 and ν_2 are the number of different molecules of ions produced by dissociation of a single molecule of solute, ν is sum of total ions $\nu = \nu_1 + \nu_2$, I is solution's ionic strength and m is the molality of the solution. The coefficients β_0, β_1 and C_ϕ are dependent on the chemical composition of solute. The values of these coefficients are tabulated by Pitzer and Mayorga (1973) for various salts. The ionic strength of the solution can be calculated using the relation: $I = 0.5 \sum m_i z_i^2$ where m_i is molality of species i and z_i is charge on the ion of that species. The value of Debye-Huckel coefficient for the osmotic function A_ϕ is 0.392 for water at 25^0C, (Brechtel & Kreidenweis, 2000).

The extrapolation of available values of osmotic coefficient for CsI from Robinson, 1937 gives the function of ϕ with molality (m) of solution. This relation, shown in equation (9) can also be used for predicting the value of ϕ for cesium Iodide.

$$\phi = 0.8481 m^{(-0.031)} \tag{9}$$

With the help of equations (3) and (6), theoretical growth factor curves with respect to relative humidity for CsI and CsOH have been generated as a part of this study. The theory of Brechtel and Kreidenweis (2000) is more relevant for predicting the theoretical growth factors of examined salts as it uses the actual solution properties such as osmotic coefficient and density.

4. Results and discussions

Growth factor is the ratio of wet diameter and initial dry diameter (D_0) of the particle. Growth factors measured for CsI and CsOH at different dry diameters were used for interpreting the growth factor curve. Reproducibility and repeatability of the data was ascertained by performing 25–30 measurement runs for each RH value performed under room temperature (typically 23 to 27 ^0C). The results are as follows:

4.1. Cesium iodide (CsI)

Fig. 2 shows the measured hygroscopic growth factors for cesium iodide particles with a dry diameter of 100 nm. The increasing and decreasing pattern of the growth factor with RH can be easily distinguished for CsI aerosols. The equilibrium size of CsI particle at a particular RH shows a dependency on its RH history. This dependency can be explained by hysteresis effect between its increasing RH and decreasing RH growth factors. Growth factor curves obtained for increasing and decreasing RH conditions were used for estimating DRH and ERH values for the test particles.

When starts from low RH, the dry CsI particles do not change their size until they reach the DRH, where a solution droplet is formed. The small growth of particles just below the DRH point is caused by water adsorption on defected sites of the lattice as described by Gysel et al. (2002) and Weingartner et al. (2002). After the DRH, further increase in relative humidity leads to particle growth by condensation and this growth is responsible for high dilution of the solution droplet which is well explained by Kohler theory.

Starting from high RH, the size of droplets decreases by evaporation of water. These droplets can also exist below the DRH in metastable equilibrium state as a supersaturated solution. Continuous decrement in relative humidity leads to crystallization of the solution droplets and lowest data point in decreasing growth factor trend provided ERH for CsI particles. The cystallization may occur

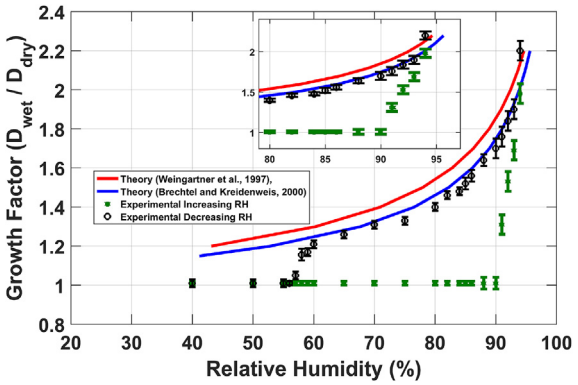

Fig. 2. Experimental and theoretical hygroscopic growth factors of 100 nm dry CsI particle

above the actual ERH of the salt due to the presence of some insoluble impurities (Gysel et al., 2002).

In addition to the experimental values, theoretical growth factor curves are also plotted in Fig. 2. These theoretical curves are based upon the equations discussed above in this paper. The agreement between the experimental values and theoretical model of Brechtel and Kreidenweis (2000) is very good within the experimental errors while the model of Weingartner et al. (1997) also captures the general trend within the proximity of experimental findings. The Brechtel and Kreidenweis (2000) model predicts the experimental results more accurately because it uses the osmotic coefficient correlation obtained for cesium iodide. Weingartner et al. (1997) model is free from the variation of osmotic coefficient, it only depends on droplet size and salt properties. The deliquescence transition point was observed at 91 ± 1% RH and is in good agreement with literature data of CRC handbook of chemistry and physics (Haynes, 2016). The experimental efflorescence relative humidity for CsI was measured at 59 ± 1% RH.

The effect of particle size on the deliquescence transition was also interpreted in this study. Fig. 3 shows the increasing RH growth factors of 50, 100, 150, 200 nm particle sizes of CsI salt. The vapor pressure over the droplet is influenced by the Kelvin effect and the Roult's law. The Kelvin effect describes the increase in the vapor pressure over a curved surface of droplet relative to a flat surface (Seinfeld and Pandis, 1998). For the larger size particles ($>100nm$), influence of the Kelvin effect on the DRH can be neglected. Measurements shows that the DRH increases with decreasing particle diameter, which is due to Kelvin effect. Insignificant difference in DRH values for CsI particles larger than 100 nm also follows the general behaviour for other salt particles e.g. NaCl (Cinkotai, 1971; Gysel et al., 2002).

4.2. Cesium hydroxide (CsOH)

In Fig. 4, the measured hygroscopic growth factors for cesium hydroxide particles with a dry diameter of 100 nm are shown. The growth factor pattern with increasing and decreasing RH can not be easily distinguished for CsOH aerosols. Measurements show that the equilibrium size of CsOH particles at a particular RH is independent from its RH history.

As shown in Fig. 4, CsOH exhibits continuous water uptake with increasing RH and no phase transition or deliquescence transition is observed. In the test RH range, CsOH particles were found to retain liquid at lower RH levels. Similar to other highly hygroscopic

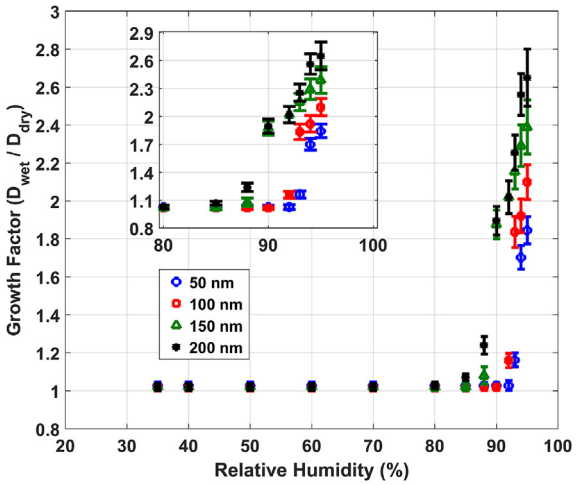

Fig. 3. Increasing RH growth factor variations for different dry sizes of CsI particle

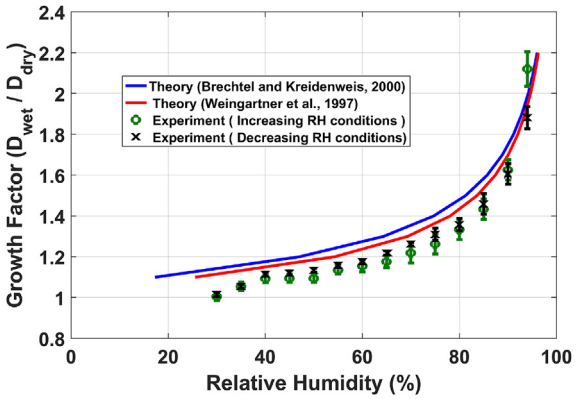

Fig. 4. Experimental and theoretical hygroscopic growth factors of 100 nm dry CsOH particle

species e.g. $NaNO_3$, complete re-crystallization is expected to occur at still lower RHs (6% for $NaNO_3$) (Gysel et al., 2002). This type of hygroscopic behaviour is also observed for some other atmospheric particles of interest such as Sodium Nitrate, Malonic acid, Glutaric Acid, Citric acid and Phthalic acid (Gysel et al., 2002; Jing et al., 2016; Peng et al., 2001; Pope, Dennis-Smither, Griffiths, Clegg, & Cox, 2010; Prenni et al., 2001).

Theoretical growth factor curves are also plotted in addition to the experimentally measured growth factors in Fig. 4. The theoretical curves are based upon modified kohler equations (Equations (3) and (6)) proposed by Weingartner et al. (1997), Brechtel and Kreidenweis (2000). The assumption taken are same as that of taken for theoretical predictions of CsI particles in this study.

Predictions of both models Weingartner et al. (1997) and Brechtel and Kreidenweis (2000) matched very well with the overall trend of experimental observations. The deviations observed at lower RH values can be seen to be reducing with RH level.

As the hysteresis effect (the dependence of the state of a system on its history) is missing in the growth factor measurements of CsOH particles, there is no significant difference between the measured growth factors of increasing (deliquescence) and decreasing (efflorescence) RH. The effect of particle size for increasing relative humidity was also examined in this study for CsOH. Fig. 5 shows the increasing RH growth factors of 50, 100, 150 and 200 nm particle sizes of CsOH salt. Measurements shows that the hygroscopic growth of CsOH particles is independent from the initial particle size at lower relative humidity. CsOH is highly hygroscopic in nature and it can absorbs water even at low relative humidities. The different size particles have approximately the same growth factors in RH range below 80%, it could be possibly due to more dominating nature of Roults law in lower RH region. Minor dependence on size at higher RH range shows that the kelvin effect is more influential/dominating in higher RH (RH > 80%) region for CsOH particles as shown in Fig. 5.

Apart from obtaining hygroscopic growth factors at subsaturated conditions, behaviour of particles in supersaturated environment is also crucial. Activation potential of CsI and CsOH aerosol particles in conjunction with growth factors cover the dynamics of water vapor with particles at all relative humidity levels. Cloud condensation nuclei counter (CCNC) can be used appropriately for characterizing water uptake behaviour of particles in supersaturated environment. The behaviour under such conditions simulates the early phase of reactor accident where steam is present in containment environment. Results of this work are mostly applicable to the later phase of reactor accident representing normal thermodynamic conditions and absence of steam.

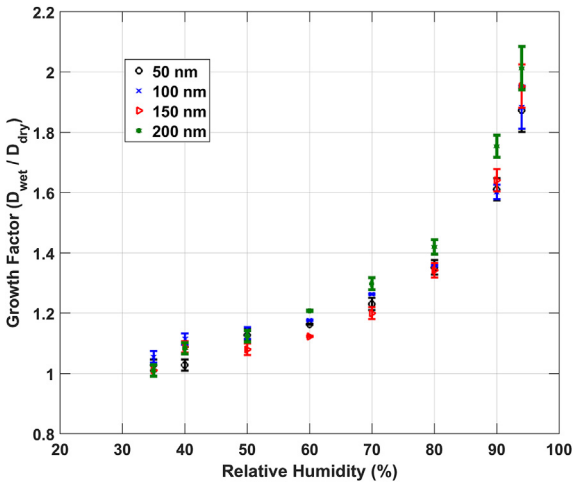

Fig. 5. Increasing RH growth factor variations different dry sizes of CsOH particle

5. Conclusions

In this study, the hygroscopic growth of laboratory generated CsI and CsOH aerosols was studied utilizing a HTDMA system. Kohler equation based theoretical models were used for predicting the hygroscopic growth curves of both type of aerosols. The dry sizes of examined salt's aerosol particles were in the range in which atmospheric particles may activate. The DRH and ERH of CsI salt were found to be 91 ± 1% and 59 ± 1% respectively. CsOH exhibits continuous water uptake and no phase transition (no DRH) was found with increasing RH. The minimum relative humidity obtained within the experimental limitations in decreasing RH measurements was not low enough for the crystallization of CsOH particles with no apparent ERH. The results indicates that the Kelvin effect is influential for the hygroscopic growth of CsI particles while the hygroscopic growth of CsOH particles was not affected by Kelvin effect. Theoretical growth factor curves were found to match the trend of the measured growth factors for both the examined salts. In the case of nuclear reactor accidents, there may be a chance of release of these water soluble compounds (i.e. CsI, CsOH) into the containment and the environment. The growth factors obtained during this study could be used as an important data in getting realistic source term or deposition rate predictions in various containment codes such as ASTEC, MELCOR or RELAP6. First time determination of DRH and ERH of CsI particles is an important contribution since it is projected to be released in significant fraction during postulated reactor accident conditions. The experimental results presented in this study fill the gap of our knowledge of hygroscopic fission product aerosol behaviour.

Acknowledgement

The present work was supported by Health, Safety and Environmental group, Bhabha Atomic Research Centre, Government of India. The authors gratefully acknowledge the financial support from the Board of Research in Nuclear Science (BRNS), Department of Atomic Energy (DAE), Government of India to conduct this research under project no. 36(2,4)/15/01/2015-BRNS. The authors also thankful to Dr. Martin Gysel, Aerosol Physics Group, Paul Scherrer Institute, Switzerland, for providing TDMAinv toolkit for HTDMA data correction.

Appendix A. Supplementary data

Supplementary data to this article can be found online at https://doi.org/10.1016/j.jaerosci.2019.03.008.

References

Acquista, N., Abramowitz, S., & Lide, D. R. (1968). Structure of the alkali hydroxides. ii. the infrared spectra of matrix–isolated csoh and csod. *The Journal of Chemical Physics, 49*(2), 780–782. https://doi.org/10.1063/1.1670139. arXiv https://doi.org/10.1063/1.1670139https://doi.org/10.1063/1.1670139.

Adachi Kouji, Z. Y. I. Y., & Mizuo, Kajino (2013). Emission of spherical cesium-bearing particles from an early stage of the fukushima nuclear accident. *Scientific Reports, 3*, 2554. https://doi.org/10.1038/srep02554https://www.nature.com/articles/srep02554#supplementary-informationhttps://doi.org/10.1038/srep02554.

Allelein, H. J., Auvinen, A., & Ball, J. (2009). *State-of-the-art report on nuclear aerosols, Vol. 5*NUCLEAR ENERGY AGENCY NEA/CSNI/R.

Amiro, B., Sheppard, S., Johnston, F., Evenden, W., & Harris, D. (1996). Burning radionuclide question: What happens to iodine, cesium and chlorine in biomass fires? *The Science of the Total Environment, 187*(2), 93–103. https://doi.org/10.1016/0048-9697(96)05125-X. http://www.sciencedirect.com/science/article/pii/004896979605125X.

Badawi, M., Xerri, B., Canneaux, S., Cantrel, L., & Louis, F. (2012). Molecular structures and thermodynamic properties of 12 gaseous cesium-containing species of nuclear safety interest: Cs2, csh, cso, cs2o, csx, and cs2x2 (x = oh, cl, br, and i). *Journal of Nuclear Materials, 420*(1), 452–462. https://doi.org/10.1016/j.jnucmat.2011.10.034. http://www.sciencedirect.com/science/article/pii/S0022311511009287.

Badger, C. L., George, I., Griffiths, P. T., Braban, C. F., Cox, R. A., & Abbatt, J. P. D. (2006). Phase transitions and hygroscopic growth of aerosol particles containing humic acid and mixtures of humic acid and ammonium sulphate. *Atmospheric Chemistry and Physics, 6*(3), 755–768. https://doi.org/10.5194/acp-6-755-2006https://www.atmos-chem-phys.net/6/755/2006.

Brechtel, F. J., & Kreidenweis, S. M. (2000). Predicting particle critical supersaturation from hygroscopic growth measurements in the humidified tdma. *Part I: Theory and sensitivity studies, Journal of the Atmospheric Sciences 57(12),* 1854–1871 arXiv:https://doi.org/10.1175/1520-0469(2000)057 < 1854:PPCSFH > 2.0.CO;2, doi:10.1175/1520-0469(2000)057 < 1854:PPCSFH > 2.0.CO;2. URL https://doi.org/10.1175/1520-0469(2000)057 < 1854:PPCSFH > 2.0.CO;2.

Buckle, E. (1991). Nucleation and growth of caesium iodide aerosols. *Journal of Aerosol Science, 22*(2), 135–147. https://doi.org/10.1016/0021-8502(91)90023-B. http://www.sciencedirect.com/science/article/pii/002185029190023B.

Camata, R. P., Hirasawa, M., Okuyama, K., & Takeuchi, K. (2000). Observation of aerosol formation during laser ablation using a low-pressure differential mobility analyzer. *Journal of Aerosol Science, 31*(4), 391–401. https://doi.org/10.1016/S0021-8502(99)00067-1. http://www.sciencedirect.com/science/article/pii/S0021850299000671.

Cinkotai, F. (1971). The behaviour of sodium chloride particles in moist air. *Journal of Aerosol Science, 2*(3), 325–329. https://doi.org/10.1016/0021-8502(71)90057-7. http://www.sciencedirect.com/science/article/pii/0021850271900577.

Clegg, S. L., & Pitzer, K. S. (1992). Thermodynamics of multicomponent, miscible, ionic solutions: Generalized equations for symmetrical electrolytes. *Journal of Physical Chemistry, 96*(8), 3513–3520. https://doi.org/10.1021/j100187a061. arXiv https://doi.org/10.1021/j100187a061https://doi.org/10.1021/j100187a061.

Cohen, M. D., Flagan, R. C., & Seinfeld, J. H. (1987). Studies of concentrated electrolyte solutions using the electrodynamic balance. 1. water activities for single-electrolyte solutions. *Journal of Physical Chemistry, 91*(17), 4563–4574. https://doi.org/10.1021/j100301a029. arXiv https://doi.org/10.1021/j100301a029https://doi.org/10.1021/j100301a029.

Duplissy, J., Gysel, M., Sjogren, S., Meyer, N., Good, N., Kammermann, L., et al. (2009). Intercomparison study of six htdmas: Results and recommendations. *Atmospheric Measurement Techniques, 2*(2), 363–378. https://doi.org/10.5194/amt-2-363-2009https://www.atmos-meas-tech.net/2/363/2009/.

Facchini, M. C., Decesari, S., Mircea, M., Fuzzi, S., & Loglio, G. (2000). Surface tension of atmospheric wet aerosol and cloud/fog droplets in relation to their organic carbon content and chemical composition. *Atmospheric Environment, 34*(28), 4853–4857. https://doi.org/10.1016/S1352-2310(00)00237-5. http://www.sciencedirect.com/science/article/pii/S1352231000002375.

Gysel, M., McFiggans, G., & Coe, H. (2009). Inversion of tandem differential mobility analyser (tdma) measurements. *Journal of Aerosol Science, 40*(2), 134–151. https://doi.org/10.1016/j.jaerosci.2008.07.013. http://www.sciencedirect.com/science/article/pii/S0021850208001778.

Gysel, M., Weingartner, E., & Baltensperger, U. (2002). Hygroscopicity of aerosol particles at low temperatures. 2. theoretical and experimental hygroscopic properties

of laboratory generated aerosols. *Environmental Science & Technology, 36*(1), 63–68. https://doi.org/10.1021/es010055g. pMID: 11811491. arXiv https://doi.org/10.1021/es010055ghttps://doi.org/10.1021/es010055g.

Gysel, M., Weingartner, E., Nyeki, S., Paulsen, D., Baltensperger, U., Galambos, I., et al. (2004). Hygroscopic properties of water-soluble matter and humic-like organics in atmospheric fine aerosol. *Atmospheric Chemistry and Physics, 4*(1), 35–50. https://doi.org/10.5194/acp-4-35-2004https://www.atmos-chem-phys.net/4/35/2004/.

Hao, W. M., Bondarenko, O. O., Zibtsev, S., & Hutton, D. (2008). Chapter 12 vegetation fires, smoke emissions, and dispersion of radionuclides in the chernobyl exclusion zone. In A. Bytnerowicz, M. J. Arbaugh, A. R. Riebau, & C. Andersen (Vol. Eds.), *Wildland fires and air pollution: Vol. 8*, (pp. 265–275). Elsevier. of Developments in Environmental Science https://doi.org/10.1016/S1474-8177(08)00012-0http://www.sciencedirect.com/science/article/pii/S1474817708000120.

Haynes, W. (2016). *CRC handbook of chemistry and physics* (97th ed.). CRC Presshttps://books.google.co.in/books?id=VVezDAAAQBAJ.

Inada, Y., & Akagane, K. (1996). Non-empirical study of chemical reactions including fission products in severe light water reactor accidents. *Journal of Nuclear Science and Technology, 33*(7), 562–568. https://doi.org/10.3327/jnst.33.562.

Jing, B., Tong, S., Liu, Q., Li, K., Wang, W., Zhang, Y., et al. (2016). Hygroscopic behavior of multicomponent organic aerosols and their internal mixtures with ammonium sulfate. *Atmospheric Chemistry and Physics, 16*(6), 4101–4118. https://doi.org/10.5194/acp-16-4101-2016https://www.atmos-chem-phys.net/16/4101/2016/.

Johnson, G., Fletcher, C., Meyer, N., Modini, R., & Ristovski, Z. (2008). A robust, portable h-tdma for field use. *Journal of Aerosol Science, 39*(10), 850–861. https://doi.org/10.1016/j.jaerosci.2008.05.005. http://www.sciencedirect.com/science/article/pii/S0021850208000992.

Jokiniemi, J. (1988). The growth of hygroscopic particles during severe core melt accidents. *Nuclear Technology, 83*(1), 16–23. https://doi.org/10.13182/NT88-A34171. arXiv https://doi.org/10.13182/NT88-A34171https://doi.org/10.13182/NT88-A34171.

Jokiniemi, J. (1990). Effect of selected binary and mixed solutions on steam condensation and aerosol behavior in containment. *Aerosol Science and Technology, 12*(4), 891–902. arXiv https://doi.org/10.1080/02786829008959401, doi:10.1080/02786829008959401https://doi.org/10.1080/02786829008959401.

Kohler, H. (1936). The nucleus in and the growth of hygroscopic droplets. *Transactions of the Faraday Society, 32*, 1152–1161. https://doi.org/10.1039/TF9363201152https://doi.org/10.1039/TF9363201152.

Kristiansen, N. I., Stohl, A., Olivié, D. J. L., Croft, B., Søvde, O. A., Klein, H., et al. (2016). Evaluation of observed and modelled aerosol lifetimes using radioactive tracers of opportunity and an ensemble of 19 global models. *Atmospheric Chemistry and Physics, 16*(5), 3525–3561. https://doi.org/10.5194/acp-16-3525-2016https://www.atmos-chem-phys.net/16/3525/2016/.

Kuczkowski, R. L., Lide, D. R., Jr., & Krisher, L. C. (1966). Microwave spectra of alkali hydroxides : Evidence for linearity of csoh and koh. *The Journal of Chemical Physics, 44*(8), 3131–3132. https://doi.org/10.1063/1.1727194. arXiv https://doi.org/10.1063/1.1727194https://doi.org/10.1063/1.1727194.

Kugeler, K., Epping, C., & Roes, J. (1989). Importance of radioactive aerosols in hypothetical high temperature reactor accidents. *Journal of Aerosol Science, 20*(8), 1421–1424. proceedings of the 1989 European Aerosol Research https://doi.org/10.1016/0021-8502(89)90852-5http://www.sciencedirect.com/science/article/pii/0021850289908525.

Leon, J. D., Jaffe, D., Kaspar, J., Knecht, A., Miller, M., Robertson, R., et al. (2011). Arrival time and magnitude of airborne fission products from the fukushima, Japan, reactor incident as measured in seattle, wa, USA. *Journal of Environmental Radioactivity, 102*(11), 1032–1038. https://doi.org/10.1016/j.jenvrad.2011.06.005. http://www.sciencedirect.com/science/article/pii/S0265931X11001366.

Li, R.-Z., Liu, C.-W., Gao, Y. Q., Jiang, H., Xu, H.-G., & Zheng, W.-J. (2013). Microsolvation of lii and csi in water: Anion photoelectron spectroscopy and ab initio calculations. *Journal of the American Chemical Society, 135*(13), 5190–5199. https://doi.org/10.1021/ja4006942. pMID: 23432353. arXiv https://doi.org/10.1021/ja4006942https://doi.org/10.1021/ja4006942.

Long, N., Truong, Y., Hien, P., Binh, N., Sieu, L., Giap, T., et al. (2012). Atmospheric radionuclides from the fukushima dai-ichi nuclear reactor accident observed in vietnam. *Journal of Environmental Radioactivity, 111*, 53–58. environmental Impacts of the Fukushima Accident (Part I) https://doi.org/10.1016/j.jenvrad.2011.11.018http://www.sciencedirect.com/science/article/pii/S0265931X1100292X.

Mariam, M. Joshi, Khandare, P., Koli, A., Khan, A., & Sapra, B. (2017). Influence of sheath air humidity on measurement of particle size distribution by scanning mobility particle sizer. *Journal of Aerosol Science, 111*, 18–25. https://doi.org/10.1016/j.jaerosci.2017.05.005. http://www.sciencedirect.com/science/article/pii/S0021850216304396.

McFarlane, J., Wren, J. C., & Lemire, R. J. (2002). Chemical speciation of iodine source term to containment. *Nuclear Technology, 138*(2), 162–178. https://doi.org/10.13182/NT138-162. arXiv https://doi.org/10.13182/NT138-162https://doi.org/10.13182/NT138-162.

McMurry, P., & Stolzenburg, M. (1989). On the sensitivity of particle size to relative humidity for los angeles aerosols. *Atmospheric Environment, 23*(2), 497–507. https://doi.org/10.1016/0004-6981(89)90593-3.

Modi, R., Khan, A., Joshi, M., Ganju, S., Singh, A., Srivastava, A., et al. (2014). Metal oxide aerosol dry deposition in laminar pipe flow at high thermal gradients and comparison with sophaeros module of astec reactor accident analysis code. *Annals of Nuclear Energy, 64*, 107–113. https://doi.org/10.1016/j.anucene.2013.09.032. http://www.sciencedirect.com/science/article/pii/S0306454913005021.

Nagai, H., Katata, G., Terada, H., & Chino, M. (2014). *Source term estimation of 131I and 137Cs discharged from the Fukushima Daiichi nuclear power plant into the atmosphere.* Tokyo: Springer Japanhttps://doi.org/10.1007/978-4-431-54583-5_15https://doi.org/10.1007/978-4-431-54583-5_15.

Onasch, T. B., Siefert, R. L., Brooks, S. D., Prenni, A. J., Murray, B., Wilson, M. A., et al. (1999). Infrared spectroscopic study of the deliquescence and efflorescence of ammonium sulfate aerosol as a function of temperature. *Journal of Geophysical Research: Atmospheres, 104*(D17), 21317–21326. https://doi.org/10.1029/1999JD900384https://doi.org/10.1029/1999JD900384.

Paliouris, G., Taylor, H., Wein, R., Svoboda, J., & Mierzynski, B. (1995). *Fire as an agent in redistributing fallout137cs in the canadian boreal forest, Science of the Total Environment 160-161.* ecological Effects of Arctic Airborne Contaminants https://doi.org/10.1016/0048-9697(95)04353-3http://www.sciencedirect.com/science/article/pii/0048969795043533.

Peng, C., Chan, M. N., & Chan, C. K. (2001). The hygroscopic properties of dicarboxylic and multifunctional acids: Measurements and unifac predictions. *Environmental Science & Technology, 35*(22), 4495–4501. https://doi.org/10.1021/es0107531. pMID: 11757607. arXiv https://doi.org/10.1021/es0107531https://doi.org/10.1021/es0107531.

Petti, D. A. (1989). Silver-indium-cadmium control rod behavior in severe reactor accidents. *Nuclear Technology, 84*(2), 128–151. https://doi.org/10.13182/NT89-A34183. arXiv https://doi.org/10.13182/NT89-A34183https://doi.org/10.13182/NT89-A34183.

Pitzer, K. S. (1973). Thermodynamics of electrolytes. i. theoretical basis and general equations. *Journal of Physical Chemistry, 77*(2), 268–277. https://doi.org/10.1021/j100621a026. arXiv https://doi.org/10.1021/j100621a026https://doi.org/10.1021/j100621a026.

Pitzer, K. S., & Mayorga, G. (1973). Thermodynamics of electrolytes. ii. activity and osmotic coefficients for strong electrolytes with one or both ions univalent. *Journal of Physical Chemistry, 77*(19), 2300–2308. https://doi.org/10.1021/j100638a009. arXiv https://doi.org/10.1021/j100638a009https://doi.org/10.1021/j100638a009.

Pope, F. D., Dennis-Smither, B. J., Griffiths, P. T., Clegg, S. L., & Cox, R. A. (2010). Studies of single aerosol particles containing malonic acid, glutaric acid, and their mixtures with sodium chloride. i. hygroscopic growth. *The Journal of Physical Chemistry A, 114*(16), 5335–5341. https://doi.org/10.1021/jp100059k. pMID: 20361768. arXiv https://doi.org/10.1021/jp100059khttps://doi.org/10.1021/jp100059k.

Prenni, A. J., DeMott, P. J., Kreidenweis, S. M., Sherman, D. E., Russell, L. M., & Ming, Y. (2001). The effects of low molecular weight dicarboxylic acids on cloud formation. *The Journal of Physical Chemistry A, 105*(50), 11240–11248. https://doi.org/10.1021/jp012427d. arXiv https://doi.org/10.1021/jp012427dhttps://doi.org/10.1021/jp012427d.

Pruppacher, H. R., Klett, J. D., & Wang, P. K. (1998). Microphysics of clouds and precipitation. *Aerosol Science and Technology, 28*(4), 381–382. arXiv https://doi.org/10.1080/02786829808965531, doi:10.1080/02786829808965531https://doi.org/10.1080/02786829808965531.

Robinson, R. A., & Stokes, R. H. (1968). *Electrolyte solutions* (2nd ed.). London: Butterworths.

Robinson, R., & Stokes (2012). *Electrolyte solutions* (Second Revised Edition). .

Sapra, B. K., Mayya, Y. S., Khan, A., Sunny, F., Ganju, S., & Kushwaha, H. S. (2008). Aerosol studies in a nuclear aerosol test facility under different turbulence

conditions. *Nuclear Technology, 163*(2), 228–244. https://doi.org/10.13182/NT08-A3983. arXiv https://doi.org/10.13182/NT08-A3983https://doi.org/10.13182/NT08-A3983.

Saraswat, S. P., Munshi, P., Khanna, A., & Allison, C. (2017). Ex-vessel loss of coolant accident analysis of iter divertor cooling system using modified relap/scadapsim/mod 4.0. 041009 *ASME, 3*(4), https://doi.org/10.1115/1.4037188 041009–13.

Saraswat, S. P., Munshi, P., Khanna, A., & Allison, C. (2018). Thermal hydraulic safety assessment of llcb test blanket system in iter using modified relap/scdapsim/mod4.0 code. *ASME, 4*(2), https://doi.org/10.1115/1.4038823 021001–10.

Seinfeld, J. H., & Pandis, S. N. (1998). *Atmospheric Chemistry and Physics from air pollution to climate change.* New York: John Wiley and Sons, Incorporated.

Shamjad, P. M., Tripathi, S. N., Aggarwal, S. G., Mishra, S. K., Joshi, M., Khan, A., et al. (2012). Comparison of experimental and modeled absorption enhancement by black carbon (bc) cored polydisperse aerosols under hygroscopic conditions. *Environmental Science & Technology, 46*(15), 8082–8089. https://doi.org/10.1021/es300295v. pMID: 22788781. arXiv https://doi.org/10.1021/es300295vhttps://doi.org/10.1021/es300295v.

Shulman, M. L., Jacobson, M. C., Carlson, R. J., Synovec, R. E., & Young, T. E. (1996). Dissolution behavior and surface tension effects of organic compounds in nucleating cloud droplets. *Geophysical Research Letters, 23*(3), 277–280. https://doi.org/10.1029/95GL03810https://doi.org/10.1029/95GL03810.

Singh, V. P., Gupta, T., Tripathi, S. N., Jariwala, C., & Das, U. (2011). Experimental study of the effects of environmental and fog condensation nuclei parameters on the rate of fog formation and dissipation using a new laboratory scale fog generation facility. *Aerosol and Air Quality Research, 11*(2), 140–154. https://doi.org/10.4209/aaqr.2010.08.0071https://doi.org/10.4209/aaqr.2010.08.0071.

Sjogren, S., Gysel, M., Weingartner, E., Baltensperger, U., Cubison, M., Coe, H., et al. (2007). Hygroscopic growth and water uptake kinetics of two-phase aerosol particles consisting of ammonium sulfate, adipic and humic acid mixtures. *Journal of Aerosol Science, 38*(2), 157–171. https://doi.org/10.1016/j.jaerosci.2006.11.005. http://www.sciencedirect.com/science/article/pii/S0021850206002096.

Stohl, A., Seibert, P., Wotawa, G., Arnold, D., Burkhart, J. F., Eckhardt, S., et al. (2012). Xenon-133 and caesium-137 releases into the atmosphere from the Fukushima Dai-ichi nuclear power plant: Determination of the source term, atmospheric dispersion, and deposition. *Atmospheric Chemistry and Physics, 12*(5), 2313–2343. https://doi.org/10.5194/acp-12-2313-2012https://www.atmos-chem-phys.net/12/2313/2012/.

Tang, I. (1976). Phase transformation and growth of aerosol particles composed of mixed salts. *Journal of Aerosol Science, 7*(5), 361–371. https://doi.org/10.1016/0021-8502(76)90022-7. http://www.sciencedirect.com/science/article/pii/0021850276900227.

Tang, I. N., & Munkelwitz, H. R. (1994). Water activities, densities, and refractive indices of aqueous sulfates and sodium nitrate droplets of atmospheric importance. *Journal of Geophysical Research: Atmospheres, 99*(D9), 18801–18808. https://doi.org/10.1029/94JD01345https://doi.org/10.1029/94JD01345.

U. N. R. Commission. (2000). *Regulatory guide 1.183 (draft was issued as DG-1081) [microform] : Alternative radiological source terms for evaluating design basis accidents at nuclear power reactors/U.S. Nuclear regulatory commission.* Washington, DC]: Office of Nuclear Regulatory Research, U.S. Nuclear Regulatory Commission, Office of Nuclear Regulatory Research.

Villani, P., Picard, D., Michaud, V., Laj, P., & Wiedensohler, A. (2008). Design and validation of a volatility hygroscopic tandem differential mobility analyzer (vh-tdma) to characterize the relationships between the thermal and hygroscopic properties of atmospheric aerosol particles. *Aerosol Science and Technology, 42*(9), 729–741. https://doi.org/10.1080/02786820802255668. arXiv https://doi.org/10.1080/02786820802255668https://doi.org/10.1080/02786820802255668.

Weingartner, E., Burtscher, H., & Baltensperger, U. (1997). Hygroscopic properties of carbon and diesel soot particles. *Atmospheric Environment, 31*(15), 2311–2327. https://doi.org/10.1016/S1352-2310(97)00023-X. http://www.sciencedirect.com/science/article/pii/S135223109700023X.

Weingartner, E., Gysel, M., & Baltensperger, U. (2002). Hygroscopicity of aerosol particles at low temperatures. 1. new low-temperature h-tdma instrument:– setup and first applications. *Environmental Science & Technology, 36*(1), 55–62. https://doi.org/10.1021/es010054o. pMID: 11811490. arXiv https://doi.org/10.1021/es010054ohttps://doi.org/10.1021/es010054o.

Wex, H., Stratmann, F., Hennig, T., Hartmann, S., Niedermeier, D., Nilsson, E., et al. (2008). Connecting hygroscopic growth at high humidities to cloud activation for different particle types. *Environmental Research Letters, 3*(3), 035004 http://stacks.iop.org/1748-9326/3/i=3/a=035004.

Wichner, R. P., & Spence, R. D. (1985). A chemical equilibrium estimate of the aerosols produced in an overheated light water reactor core. *Nuclear Technology, 70*(3), 376–393. https://doi.org/10.13182/NT85-A15964. arXiv https://doi.org/10.13182/NT85-A15964https://doi.org/10.13182/NT85-A15964.

Wise, M. E., Surratt, J. D., Curtis, D. B., Shilling, J. E., & Tolbert, M. A. (2003). Hygroscopic growth of ammonium sulfate/dicarboxylic acids. *Journal of Geophysical Research: Atmospheres, 108*(D20), https://doi.org/10.1029/2003JD003775. n/a–n/a, 4638 https://doi.org/10.1029/2003JD003775.

Yoschenko, V., Kashparov, V., Levchuk, S., Glukhovskiy, A., Khomutinin, Y., Protsak, V., et al. (2006). Resuspension and redistribution of radionuclides during grassland and forest fires in the chernobyl exclusion zone: Part ii. Modeling the transport process. *Journal of Environmental Radioactivity, 87*(3), 260–278. https://doi.org/10.1016/j.jenvrad.2005.12.003. http://www.sciencedirect.com/science/article/pii/S0265931X05003309.